

## Liquid Crystals

# Ion-Pairing Chromonic Liquid Crystals via Alternately Stacked Assembly of Amphiphilic Charged $\pi$ -Electronic Systems

Yuto Maruyama, Koji Harano, Hayato Kanai, Yasuhiro Ishida, Hiroki Tanaka, Shinya Sugiura, and Hiromitsu Maeda\*

**Abstract:** In this study, a new assembly strategy for lyotropic chromonic liquid crystals (LCLCs) is proposed using  ${}^i\pi$ - ${}^j\pi$  interactions, mainly comprising electrostatic and dispersion forces, between charged  $\pi$ -electronic systems to form stacking structures supported by the hydration of triethylene glycol (TEG) units. The *meso*-TEG-aryl-substituted porphyrin Au<sup>III</sup> complex, an amphiphilic  $\pi$ -electronic cation, showed diverse states and assembly modes in ion pairs depending on the coexisting counteranions. The PCCp<sup>-</sup> ion pair formed a hexagonal columnar (Col<sub>h</sub>) LC phase based on a charge-by-charge assembly, suggesting the formation of an ordered arrangement of charged  $\pi$ -electronic systems through  ${}^i\pi$ - ${}^j\pi$  interactions, with reduced interactions between the TEG chains. Furthermore, in the presence of water, LCLC behavior in the Col<sub>h</sub> and nematic columnar phases according to the amount of water were observed for the PCCp<sup>-</sup> ion pair as a result of  ${}^i\pi$ - ${}^j\pi$  interactions. Magnetic-field-induced orientation of the charge-by-charge columnar structures upon dehydration was observed. Furthermore, single-stranded charge-by-charge columnar structures, as components of the LCLCs, were observed using transmission electron microscopy (TEM).

## Introduction

The molecular states can be controlled by solvation. Monomeric states were observed in well-solubilizing solvents, whereas crystallization occurs in poor solvents.<sup>[1]</sup> Appropriate modulation of the interactions between molecules and solvents results in the formation of aggregates dispersed in solutions<sup>[2]</sup> and, in some cases, supramolecular gels by capturing solvent molecules in entangled fiber and sheet structures.<sup>[3]</sup> More dynamically assembled states, including solvents, are lyotropic liquid crystals (LLCs), wherein the hydrophobic effects between the amphiphilic molecules form aggregates.<sup>[4]</sup> In particular, LLCs comprising  $\pi$ -electronic systems such as dyes and nucleic acids are lyotropic chromonic liquid crystals (LCLCs). In LCLC phases, the molecules are stacked not only by hydrophobic effects but also by  $\pi$ - $\pi$  interactions. In contrast to conventional amphiphilic mesophases with critical micelle concentrations (CMC), the assemblies that form LCLCs have no clear critical concentrations, and constituent molecules reversibly form stacking structures (Figure 1a).<sup>[5]</sup> Würthner et al. reported the self-assembling perylene bisimide dyes bearing oligo(ethylene glycol) units in water to obtain thermally responsive functional nanostructures.<sup>[6]</sup>  $\pi$ -Electronic systems bearing charged peripheral substituents, such as perylene bisimides,<sup>[7]</sup> phthalocyanines,<sup>[8]</sup> and porphyrins,<sup>[9]</sup> have also been used as mesogens for LCLCs.

The ionic moieties of the mesogens and the corresponding counterions act as units to enhance the affinities for water molecules. The core  $\pi$ -electronic units form stacked assemblies via dispersion forces, resulting in LCLCs. Electrostatic interactions between the charged peripheral substituents also support the stacking of mesogens.<sup>[9]</sup> In contrast, there are a few examples of  $\pi$ -electronic systems whose charges are delocalized in the core to form stacking structures for LCLCs, where the counterions of the charged  $\pi$ -electronic systems are located outside the columnar structures.<sup>[10]</sup> Another assembly strategy for LCLCs involves the use of the electrostatic forces between charged  $\pi$ -electronic systems to form stacked structures. Alternately stacked  $\pi$ -electronic cations and anions form charge-by-charge assemblies mainly via electrostatic and dispersion forces, that is,  ${}^i\pi$ - ${}^j\pi$  interactions (Figure 1b).<sup>[11,12]</sup> Such ion-pairing assemblies comprising charged  $\pi$ -electronic systems have been observed in crystals, supramolecular gels, and thermotropic liquid crystals depending on the peripheral substituents.<sup>[13]</sup> However, LCLCs based on charge-by-charge assemblies, through introducing hydrophilic substituents,

[\*] Y. Maruyama, Dr. H. Tanaka, Dr. S. Sugiura, Prof. H. Maeda  
 Department of Applied Chemistry, College of Life Sciences  
 Ritsumeikan University  
 Kusatsu 525-8577, Japan  
 E-mail: maedahir@ph.ritsumei.ac.jp

Dr. K. Harano  
 Center for Basic Research on Materials  
 National Institute for Materials Science  
 Tsukuba 305-0044, Japan

Dr. K. Harano  
 Research Center for Autonomous Systems Materialogy, Institute of  
 Integrated Research  
 Institute of Science Tokyo  
 Yokohama 226-8501, Japan

Dr. H. Kanai, Dr. Y. Ishida  
 Center for Emergent Matter Science (CEMS), RIKEN  
 Wako 351-0198, Japan

© 2024 The Authors. Angewandte Chemie International Edition published by Wiley-VCH GmbH. This is an open access article under the terms of the Creative Commons Attribution License, which permits use, distribution and reproduction in any medium, provided the original work is properly cited.

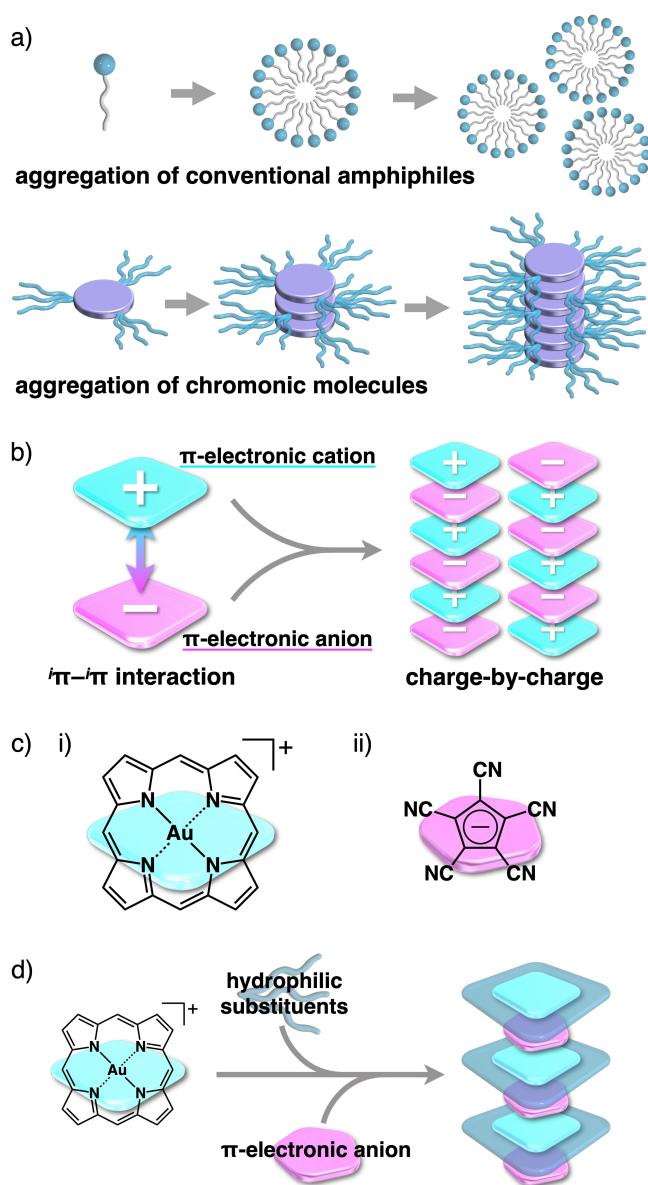


**Figure 1.** a) Aggregation modes of conventional amphiphiles and chromonic molecules in water, b) assemblies of  $\pi$ -electronic cations and anions, c) i) porphyrin  $\text{Au}^{\text{III}}$  complexes, represented as a parent structure, and ii)  $\text{PCCp}^-$  as building units of ion-pairing assemblies, and d) introduction of hydrophilic substituents into porphyrin  $\text{Au}^{\text{III}}$  complexes to form amphiphilic ion-pairing assemblies.

have not been reported due to the absence of appropriate amphiphilic  $\pi$ -electronic ions.

The potential positively charged core units of LCLCs are porphyrin  $\text{Au}^{\text{III}}$  complexes that form various assemblies in combination with anions (Figure 1c i).<sup>[14]</sup> The complexation of  $\text{Au}^{\text{III}}$  ( $d^8$ ) by porphyrins as dianionic ligands is crucial for preparing large charged  $\pi$ -planes, which effectively form tightly stacked ion pairs and the resulting assembling structures. Notably, ion pairs with pentacyanocyclopentadienide ( $\text{PCCp}^-$ )<sup>[13d,15]</sup> (Figure 1c ii) as a  $\pi$ -electronic anion exhibited charge-by-charge assemblies in the form of supramolecular gels and thermotropic liquid crystals.<sup>[14a]</sup>

Given the previous studies, a potential strategy for forming ion-pairing LCLCs involves the introduction of hydrophilic substituents into porphyrin  $\text{Au}^{\text{III}}$  complexes (Figure 1d). In this study, the ion-pairing assemblies of an amphiphilic porphyrin  $\text{Au}^{\text{III}}$  complex with counteranions were investigated. The introduction of a charged  $\pi$ -electronic system as a counteranion of the amphiphilic  $\pi$ -electronic cation results in the formation of LCLCs, exhibiting a magnetic-field-induced orientation, and single-stranded charge-by-charge assembly via the synergistic use of  $\pi$ - $\pi$  interactions and hydrophobic effects.

## Results and Discussion

Assembly in aqueous media requires hydrophilic ionic and nonionic substituents for hydration such as  $\text{CH}_3$ - $(\text{OCH}_2\text{CH}_2)_3\text{O}$  (triethylene glycol, TEG) moieties for the latter. Amphiphilic porphyrin  $\text{Au}^{\text{III}}$  complex **1** (**Figure 2**) as a  $\text{Cl}^-$  ion pair was synthesized by  $\text{Au}^{\text{III}}$  complexation of 3,4,5-tris(TEG)-substituted arylporphyrin<sup>[16]</sup> **1** using  $\text{KAuCl}_4 \cdot n\text{H}_2\text{O}$  and  $\text{NaOAc} \cdot 3\text{H}_2\text{O}$  in  $\text{AcOH}$ .  $\text{PCCp}^-$  as a desired counteranion and  $\text{B}(\text{C}_6\text{F}_5)_4^-$  as a reference were introduced by the ion-pair metathesis of **1** ( $\text{Au}^{\text{III}}$ ) using  $\text{NaPCCp}^-$  and  $\text{LiB}(\text{C}_6\text{F}_5)_4$ , respectively (Figure 2). The ion pairs were characterized using  $^1\text{H}$  and  $^{13}\text{C}$  NMR and ESI-MS. In  $\text{CDCl}_3$  (1 mM) at  $20^\circ\text{C}$ , the  $^1\text{H}$  NMR signals of  $\beta$ -CH (9.43 ppm) and aryl-CH (7.69 ppm) of **1** ( $\text{Au}^{\text{III}}$ ) in **1** ( $\text{Au}^{\text{III}}$ )- $\text{PCCp}^-$  were found to be shifted downfield compared to those of **1** ( $\text{Au}^{\text{III}}$ )- $\text{Cl}^-$  (9.32 and 7.48 ppm, respectively), suggesting that  $\beta$ -CH and aryl-CH were located out of the  $\pi$ -plane of  $\text{PCCp}^-$  in the stacked ion pair ( $\pi$ - $\text{slip}$ ) (Figure S2,4). The  $^1\text{H}$  NMR signal of the aryl-CH of **1** ( $\text{Au}^{\text{III}}$ ) in **1** ( $\text{Au}^{\text{III}}$ )- $\text{PCCp}^-$  was broader because of hydrogen-bonding interactions with the CN sites of  $\text{PCCp}^-$ .

UV/Vis absorption spectra with the maxima ( $\lambda_{\text{max}}$ ), as those of the Soret bands, at 425 nm in  $\text{CH}_2\text{Cl}_2$  were observed for **1** ( $\text{Au}^{\text{III}}$ )- $\text{Cl}^-$  and **1** ( $\text{Au}^{\text{III}}$ )- $\text{PCCp}^-$ , suggesting that counteranions had no influence (Figure 3). These observations suggest that the ion pairs exist in dispersed states without aggregation. In contrast, in aqueous solution (8  $\mu\text{M}$ ), **1** ( $\text{Au}^{\text{III}}$ )- $\text{Cl}^-$  and **1** ( $\text{Au}^{\text{III}}$ )- $\text{PCCp}^-$  exhibited blue-shifted absorptions at 415 and 419 nm, respectively (Figure 3). The differences

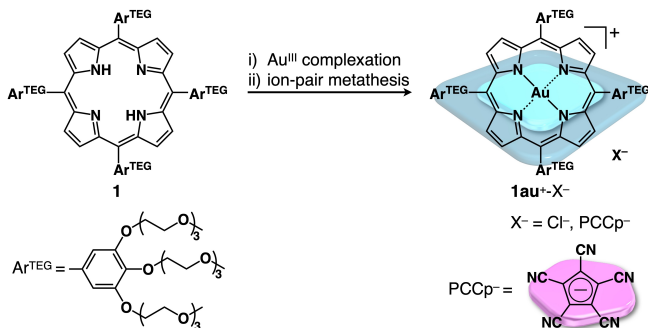


**Figure 2.** Synthesis of the amphiphilic porphyrin  $\text{Au}^{\text{III}}$  complex as ion pairs.

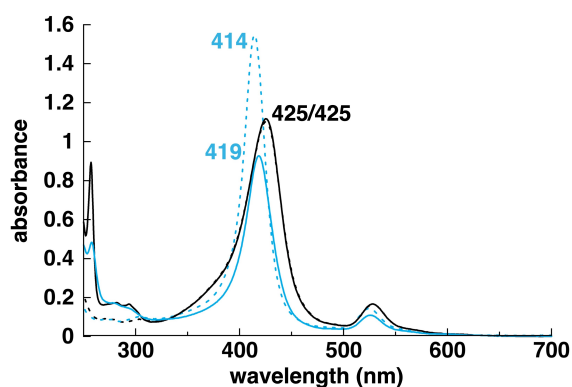


**Figure 3.** UV/Vis absorption spectra of  $1\text{au}^+-\text{Cl}^-$  (broken line) and  $1\text{au}^+-\text{PCCp}^-$  (solid line) in  $\text{CH}_2\text{Cl}_2$  (black) and aqueous solution (blue) ( $8\ \mu\text{M}$  for each).

between the blue shifts can be ascribed to the different assembly modes according to the coexisting anions. The moderate blue shift (6 nm) for  $1\text{au}^+-\text{PCCp}^-$  would be derived from the smaller exciton coupling between  $1\text{au}^+$  units separated with an approximate distance of ca. 0.7 nm in a charge-by-charge assembly. Oppositely charged  $\pi$ -systems in  $1\text{au}^+-\text{PCCp}^-$  induce effective  $i\pi$ - $i\pi$  interactions, supported by hydrophobic effects. In contrast, the larger blue shift of  $1\text{au}^+-\text{Cl}^-$  (10 nm) can be attributed to the stacked  $1\text{au}^+$  units. Hydration for  $\text{Cl}^-$  could be used for the stacking arrangement of  $1\text{au}^+$ .<sup>[17]</sup> Furthermore, in an aqueous solution, the ion pairs formed dispersed assembled structures with sizes of ca. 500 nm, as indicated by DLS measurements (Figure S12). Observations in aqueous solutions suggest that the electrostatic forces in the  $\text{PCCp}^-$  ion pair are used for assembly but not for hydration.<sup>[18]</sup>

Bulk-state assembled structures were examined for ion pairs. The viscous liquid-state  $1\text{au}^+-\text{Cl}^-$ , prepared from  $\text{CH}_2\text{Cl}_2$ , showed a synchrotron X-ray diffraction (XRD) pattern derived from the amorphous state at r.t. (Figure 4a). In contrast, differential scanning calorimetry (DSC) of  $1\text{au}^+-\text{PCCp}^-$  suggested the transitions at  $-9$  and  $267^\circ\text{C}$  (heating) and  $258$  and  $-18^\circ\text{C}$  (cooling) (Figure S15). The wide temperature range of the mesophase is characteristic of the  $\text{PCCp}^-$  ion pairs of porphyrin  $\text{Au}^{\text{III}}$  complexes.<sup>[14a]</sup> Dendritic-like polarized optical microscopy (POM) textures, which are generally ascribable to columnar phases formed by molecular aggregates, were observed at  $20^\circ\text{C}$  (Figure 4b i). Synchrotron XRD at  $-30^\circ\text{C}$  showed the complex diffraction pattern of  $d=2.28$  (110), 1.91 (200), 1.44 (020), 1.14 (220), 0.94 (400), 0.80 (420), 0.77 (330), 0.75 (510), 0.72 (040), 0.68 (001), 0.66 (240), 0.63 (600), 0.59 (530), 0.58 (440), and 0.34 (002) nm revealed a rectangular columnar ( $\text{Col}_r$ ) structure with  $a=3.81$  nm,  $b=2.84$  nm, and  $c=0.68$  nm ( $Z=2$  for  $\rho=1.32$ ) (Figure S37k). On the other hand, at  $20^\circ\text{C}$ , the synchrotron XRD pattern of  $d=2.22$  (100), 1.27 (110), 1.10 (200), 0.83 (210), 0.73 (300), 0.69 (001), 0.64 (220), and 0.61 (310) nm revealed a hexagonal columnar ( $\text{Col}_h$ ) structure with  $a=2.56$  nm and  $c=0.69$  nm ( $Z=1$  for  $\rho=1.25$ ) (Figure 4b ii). As indicated by the  $a$  value, the constituent size was consistent with the model structure of  $1\text{au}^+$ . In contrast,

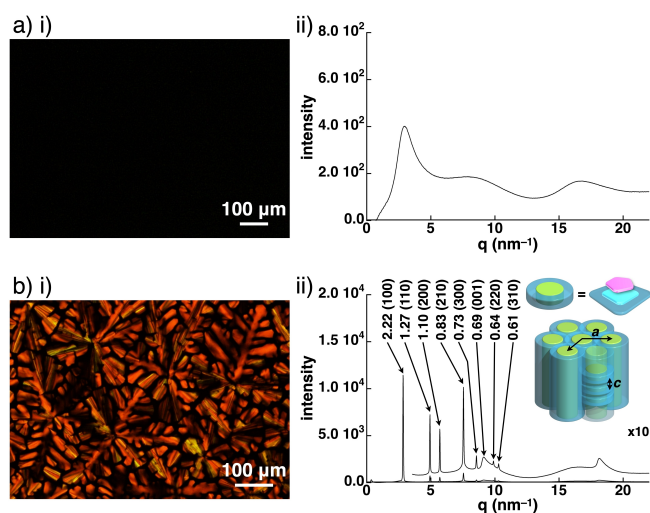


**Figure 4.** i) POM images and ii) synchrotron XRD of a)  $1\text{au}^+-\text{Cl}^-$  at  $25^\circ\text{C}$  and b)  $1\text{au}^+-\text{PCCp}^-$  at  $20^\circ\text{C}$  upon cooling. The examined samples were water-free ion pairs.

the  $c$  value indicated an alternately stacked ion-pairing structure in the charge-by-charge assembly mode. The  $\text{Col}_h$  phase was observed below ca.  $260^\circ\text{C}$  without any transitions. The states of  $1\text{au}^+-\text{Cl}^-$  and  $1\text{au}^+-\text{PCCp}^-$  were distinct depending on the coexisting anions. In the assemblies of  $1\text{au}^+-\text{PCCp}^-$ , the hydrophilic side chains contribute little to the aggregation, mainly attributed to the  $i\pi$ - $i\pi$  interactions between  $1\text{au}^+$  and  $\text{PCCp}^-$  and hydrophobic effects.

The assembly behavior was further examined for ion pair  $1\text{au}^+-\text{PCCp}^-$  in the presence of water. The water-containing  $1\text{au}^+-\text{PCCp}^-$ , in the percentages (w/w) of ion pairs to the total amounts (ion-pair percentages) of 75%–1%, were prepared for the examinations. The POM textures at r.t. varied depending on the ion-pair percentages (Figure 5a). The samples with ion-pair percentages of 75%, 50%, and 40%,  $1\text{au}^+-\text{PCCp}^-_{75\%/50\%/40\%}$  labeled with the corresponding percentages, exhibited  $\text{Col}_h$  structures via synchrotron XRD at r.t., whereas  $1\text{au}^+-\text{PCCp}^-_{35\%}$  and the samples with higher amounts of water showed no diffraction peaks from the periodic arrangement of the columns (Figure 5b). The  $a$  values of  $1\text{au}^+-\text{PCCp}^-_{75\%/50\%/40\%}$  were estimated to be 2.72, 3.12, and 3.13 nm, respectively, suggesting that the intercolumnar distances were extended by more effective hydration at the TEG chains. The diffractions at 0.68, 0.76, and 0.82 nm, respectively, suggested the formation of charge-by-charge assemblies in the presence of water. These observations indicated that  $1\text{au}^+-\text{PCCp}^-$  in the  $\text{Col}_h$  phases exhibited LCLC behaviors based on the interactions between oppositely charged  $\pi$ -electronic systems. More water interfered with the ordered arrangement of the columnar structures.  $1\text{au}^+-\text{PCCp}^-_{35\%/30\%/25\%/20\%}$  formed a nematic columnar ( $\text{N}_{\text{col}}$ ) phase with only orientational ordering (Figure 5c).  $1\text{au}^+-\text{PCCp}^-_{15\%/10\%/1\%}$  showed no POM textures, indicating that the ion-pair columns were isotropically dispersed and non-LCLC states, labeled as  $\text{Iso}_{\text{col}}$  in this study, at r.t. (Figure 5c). The diffractions, some of which

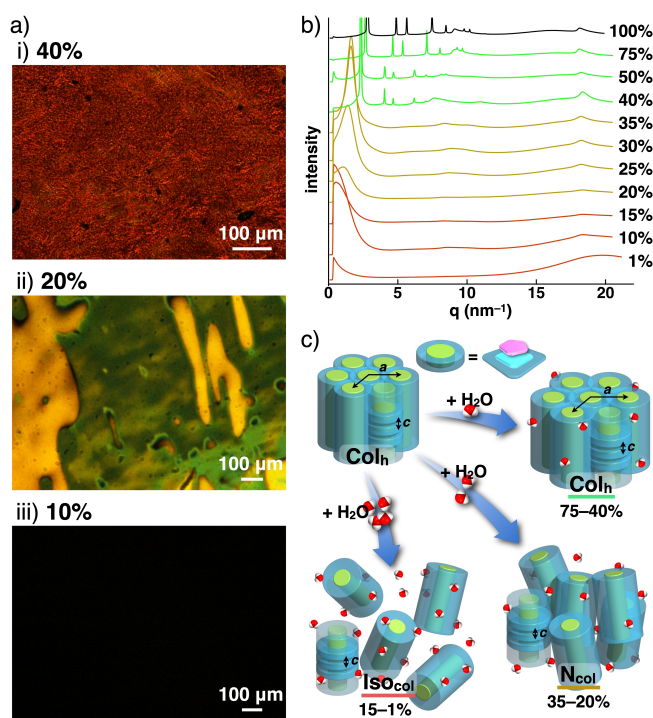


**Figure 5.** a) POM images of i)  $1\text{au}^+\text{-PCCp}^-_{40\%}$ , ii)  $1\text{au}^+\text{-PCCp}^-_{20\%}$ , and iii)  $1\text{au}^+\text{-PCCp}^-_{10\%}$  at  $20^\circ\text{C}$ , b) synchrotron XRD of  $1\text{au}^+\text{-PCCp}^-$  and water-containing  $1\text{au}^+\text{-PCCp}^-$  at  $25^\circ\text{C}$ , and c) phase changes according to the ion-pair percentages.

were weak and not observed, at ca. 0.76 nm suggested the retaining charge-by-charge assemblies.

The assembly modes in the LCLCs of  $1\text{au}^+\text{-PCCp}^-$  were modulated by the thermal conditions and concentrations (Figure 6a). For example, the thermal transitions of  $1\text{au}^+\text{-PCCp}^-_{40\%}$  were examined by DSC and POM, showing transitions at  $50$  and  $64^\circ\text{C}$ , the former of which was indicated only by POM. Synchrotron XRD revealed  $\text{Col}_h$  and  $\text{Col}_h'$  phases with  $a$  values of  $3.19$  and  $2.93$  nm and  $c$  values of  $0.82$  and  $0.80$  nm at  $50$  and  $70^\circ\text{C}$ , respectively, upon heating, whereas no diffraction peaks from the periodic arrangement of the columns ( $c=0.81$  nm) were observed at  $60^\circ\text{C}$ . The POM texture at  $60^\circ\text{C}$  suggests that the  $\text{N}_{\text{col}}$  phase was formed within a small temperature range. At  $<64^\circ\text{C}$ , intercolumnar distances and ordering were mainly controlled by thermal motion. At  $64^\circ\text{C}$ , intercolumnar distances were changed due to deswelling by partial dehydration upon heating. However, because hydration upon cooling was difficult, columnar structures of different sizes and phases were formed in domains with different concentrations.<sup>[19]</sup>

$1\text{au}^+\text{-PCCp}^-_{35\%/30\%/25\%/20\%}$  in  $\text{N}_{\text{col}}$  phases at r.t. showed thermal transitions to optically isotropic states, as observed in  $1\text{au}^+\text{-PCCp}^-_{15\%/10\%/1\%}$  at r.t., and to POM-active states, such as  $1\text{au}^+\text{-PCCp}^-_{40\%}$ . For example,  $1\text{au}^+\text{-PCCp}^-_{20\%}$  exhibited thermal transitions at  $40$  and  $67^\circ\text{C}$ . At  $70^\circ\text{C}$ ,  $1\text{au}^+\text{-PCCp}^-_{20\%}$  showed the  $\text{Col}_h'$  phase, upon dehydration, with  $a$  and  $c$  values of  $2.96$  and  $0.70$  nm, respectively, as revealed by synchrotron XRD. This observation suggested that the

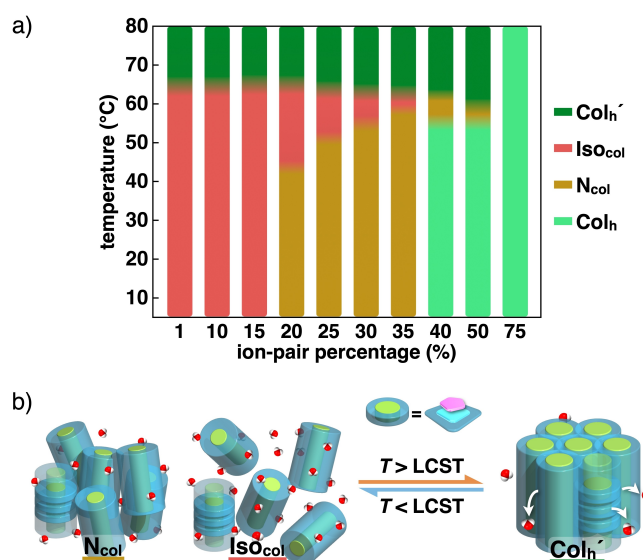


**Figure 6.** a) Diagram of phase changes of water-containing  $1\text{au}^+\text{-PCCp}^-$  by thermal transitions and b) assembly behavior model at LCST. In a), the areas of light green, yellow, red, and dark green refer to  $\text{Col}_h$ ,  $\text{N}_{\text{col}}$ , isotropically dispersed columnar ( $\text{Iso}_{\text{col}}$ ) phases, and  $\text{Col}_h'$  phase due to deswelling by dehydration, respectively.

phase between  $40$  and  $67^\circ\text{C}$  would be an  $\text{Iso}_{\text{col}}$  phase. Similar behavior was observed in  $1\text{au}^+\text{-PCCp}^-_{35\%/30\%/25\%}$  with lower  $\text{N}_{\text{col}}\text{-Iso}_{\text{col}}$  transition temperatures at lower concentrations. On the other hand, in  $1\text{au}^+\text{-PCCp}^-_{35\%/30\%/25\%}$ , decreasing the solubility at  $5^\circ\text{C}$  upon cooling resulted in the precipitation of  $\text{Col}_h$  structures with  $a=3.85\text{--}3.95$  nm and  $c=0.72\text{--}0.75$  nm ( $Z=1$  for  $\rho=0.51$ ). Further diluted  $1\text{au}^+\text{-PCCp}^-_{15\%/10\%/1\%}$  in  $\text{Iso}_{\text{col}}$  phases at r.t. showed transitions to  $\text{Col}_h'$  states upon partial dehydration at  $63$ ,  $59$ , and  $62^\circ\text{C}$ , respectively. The transitions caused by the changes in molecular motion were not observed in the range of  $5\text{--}60^\circ\text{C}$  because each columnar structure was dispersed in  $\text{Iso}_{\text{col}}$ . At  $\leq 35\%$  ion-pair percentages, thermal motion mainly controlled the intercolumnar distances and ordering below the transition temperatures to the partially dehydrated  $\text{Col}_h'$  states. Notably, the  $c$  values in the columns were observed at  $0.69\text{--}0.76$  nm except for  $1\text{au}^+\text{-PCCp}^-_{1\%}$ , whose stacking was disordered due to the smaller interactions between the side chains in the columns. In the  $60\text{--}70^\circ\text{C}$  range, deswelling by partial dehydration upon heating resulted in phase transitions to the  $\text{Col}_h'$  phase, whereas swelling by hydration upon cooling induced the phase transitions to less ordered phases for the states with ion-pair percentages of  $\leq 35\%$ . These observations indicate the presence of lower critical solution temperatures (LCST) for the partially dehydrated  $\text{Col}_h'$  states except for  $1\text{au}^+\text{-PCCp}^-_{75\%}$  (Figure 6b).<sup>[20]</sup>

In contrast to the  $\text{PCCp}^-$  ion pair, water-containing  $1$  ( $1_{75\%/50\%/25\%}$ ) and  $1\text{au}^+\text{-Cl}^-$  ( $1_{75\%/50\%/25\%}$ ) exhibited no LCLCs (Figure S14,15,18–23,37–42). Thermal transitions of  $1_{75\%/50\%/25\%}$  were examined by DSC analysis, showing that the transitions generally corresponded to the changes in optical microscopy images due to aggregation by dehydration upon heating and disaggregation by hydration upon

cooling. The observed aggregates were isotropic and formed via hydrophobic effects. Furthermore,  $1\text{au}^+-\text{Cl}^-_{75\%/50\%/25\%}$  showed no thermal transitions in DSC analysis and almost no dehydration upon heating. Electrostatic repulsion between  $1\text{au}^+$  in the absence of efficiently stackable anions in  $1\text{au}^+-\text{Cl}^-$  prevented the formation of aggregates. These results suggest that  $\pi-\pi$  interactions, as observed in  $1\text{au}^+-\text{PCCp}^-$ , are crucial for the formation of LCLCs.

Taking advantage of the anisotropic magnetic susceptibility of  $1\text{au}^+-\text{PCCp}^-$  owing to its columnar structure and viscosity tunability by controlling the water content, a macroscopically oriented structure could be stably constructed.<sup>[21]</sup> The  $\text{Col}_h$  structure fabricated under the slow condensation of  $1\text{au}^+-\text{PCCp}^-_{10\%}$  drop-cast on a glass substrate to dryness by vaporizing water for ca. 3 h showed no orientation (Figure 7a, S66a). In contrast, for  $1\text{au}^+-\text{PCCp}^-_{10\%}$  placed in a 10-T magnetic field applied along the glass substrate under the similar drying procedure, the sample was initially less viscous and responsive to the magnetic field, whereas, in the end, it became viscous enough to maintain the oriented structure even without the magnetic field. When the resulting sample was observed using POM while changing its angular geometry, the brightness was changed homogeneously and drastically throughout the region, indicating that the columns were oriented in one direction along the glass substrate (Figure S66b).<sup>[21a]</sup> Although this result could not tell whether the columns preferred to orient parallel or perpendicular to the magnetic field, the 2D XRD measurement detected anisotropic diffractions due to the alternately stacked ion-pairing structure, that is, the (001) and (002) faces, specifically in the equatorial region (Figure 7b), which allowed us to conclude that the columns were oriented perpendicular to the magnetic field.<sup>[21d]</sup> Encouraged by the successful horizontal orientation of the columns, a vertical orientation was also attempted. In this case, the same condensation process was performed under a 10-T magnetic field with the glass substrate rotated in-plane at 20 rpm.<sup>[21c]</sup> Accordingly, the

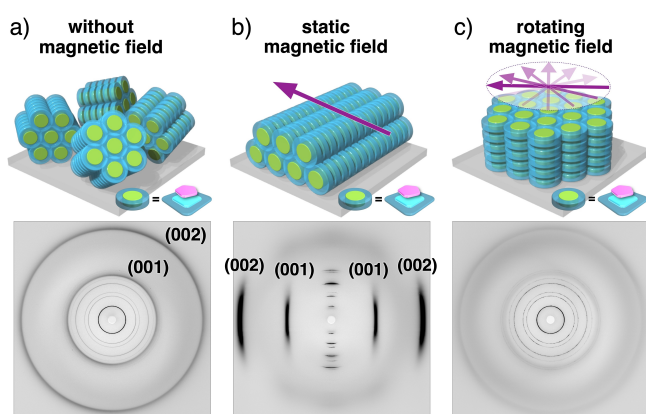


**Figure 7.** 2D XRD images of the samples of  $1\text{au}^+-\text{PCCp}^-$  cast on glass substrates, which were prepared by slow vaporization of water from  $1\text{au}^+-\text{PCCp}^-_{10\%}$  a) without a magnetic field, b) with a 10-T static magnetic field applied along the glass substrate, and c) with a 10-T magnetic field rotating in-plane of the glass substrate.

sample was virtually exposed to an in-plane rotating magnetic field, which forced the columns to orient perpendicular to the rotation plane. Indeed, the resulting sample exhibited weak angle-independent birefringence in the POM observations, consistent with the general tendency for vertically oriented columnar liquid crystals (Figure S66c).<sup>[21b]</sup> In addition, the resulting sample hardly exhibits the diffraction of the (001) and (002) faces because of the alternately stacked ion-pairing structure, further supporting the vertical orientation of the columns, where the periodicity along the column axis cannot exhibit the corresponding diffraction (Figure 7c). Overall,  $1\text{au}^+-\text{PCCp}^-$  with an alternately stacked ion-pairing structure can be unidirectionally oriented on demand over a macroscopic scale.

Single-stranded charge-by-charge assemblies were observed by transmission electron microscopy (TEM) in a non-stained specimen prepared from a more dilute aqueous solution of  $1\text{au}^+-\text{PCCp}^-$  (0.1 mM) and deposited on a thin carbon film via freeze-drying processes (Figure 8a), suggesting the importance of charge-by-charge assemblies in LCLCs for the fabrication of ordered structures. The widths of 3.7–4.0 nm at the thinnest parts indicated the single strands of charge-by-charge assemblies that are isolated without bundling. The corresponding high-angle annular dark-field scanning TEM (HAADF-STEM) image also showed a high image contrast of the assembly, suggesting

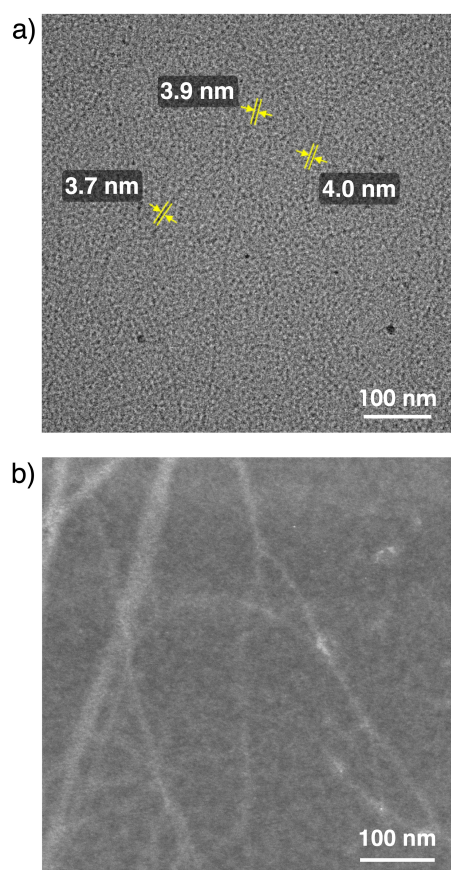


**Figure 8.** a) TEM and b) HAADF-STEM images of the single strands of  $1\text{au}^+-\text{PCCp}^-$  formed in aqueous solutions (0.1 mM).

the presence of heavy Au atoms in the single strands (Figure 8b). The width of the simulated single-stranded charge-by-charge assembly comprising  $1\text{Au}^+\text{-PCCp}^-$  units was 3.9 nm and is consistent with the observed TEM images (Figure S67).<sup>[22]</sup> The direct observation of single-stranded charge-by-charge assemblies formed by  ${}^i\pi\text{-}^j\pi$  interactions suggests that the synergetic use of electrostatic and dispersion forces is effective for producing polymer structures. More concentrated conditions induce the formation of LCLCs with water molecules acting as connectors between charge-by-charge columnar structures.

## Conclusion

This study demonstrated the synthesis of amphiphilic porphyrin  $\text{Au}^{\text{III}}$  complex ion pairs for the assembly in the absence and presence of water. In the  $\text{PCCp}^-$  ion pair, synchrotron XRD revealed the formation of thermotropic liquid crystals arranged in a charge-by-charge assembly based on  ${}^i\pi\text{-}^j\pi$  interactions. In the presence of water, LCLC behaviors, in the charge-by-charge-based  $\text{Col}_h$  and  $\text{N}_{\text{col}}$  phases, along with  $\text{Iso}_{\text{col}}$  phases were observed according to the amounts of water and the temperatures. Oriented charge-by-charge columnar assemblies in the  $\text{Col}_h$  phase were formed from an aqueous solution by drying under a magnetic field. Furthermore, as observed by TEM, single-stranded charge-by-charge assemblies as components of LCLCs were formed in a diluted aqueous solution via freeze-drying processes. These observations suggest that the charges in the  $\text{PCCp}^-$  ion pair were used for assembly via  ${}^i\pi\text{-}^j\pi$  interactions but not for hydration. This study also demonstrates a new type of amphotropic LCs<sup>[23]</sup> based on charged  $\pi$ -electronic systems. Further modifications of amphiphilic charged  $\pi$ -electronic systems, such as the partial introduction of hydrophilic *meso*-aryl moieties, would result in solvent-supported highly ordered assembled structures that are responsive to external stimuli. The assembly modes and properties can also be modulated by combining with  $\pi$ -electronic anions.

## Acknowledgements

This work was supported by JSPS KAKENHI Grant Numbers JP18H01968, JP22H02067, and JP23K23335 for Scientific Research (B), JP23K17951 for Challenging Research (Exploratory), JP20J22745 for JSPS Fellows, JP20H05863 for Transformative Research Areas (A) “Condensed Conjugation”, and JP23H04874 for Transformative Research Areas (A) “Materials Science of Meso-Hierarchy”, Ritsumeikan Global Innovation Research Organization (R-GIRO) project (2017–22 and 2022–27), and JST SPRING Grant Number JPMJSP2101. Theoretical calculations were partially performed at the Research Center for Computational Science, Okazaki, Japan (Projects: 21-IMS-C077, 22-IMS-077, 23-IMS-069). The synchrotron radiation experiments were performed at the BL40B2 (2021B1828, 2022A1689, 2022B1546, 2023A1331) of SPring-8 with the

approval of the Japan Synchrotron Radiation Research Institute (JASRI) and at the BL05XU with the approval of RIKEN. We thank Prof. Hitoshi Tamiaki, Ritsumeikan University, for various measurements.

## Conflict of Interest

The authors declare no conflict of interest.

## Data Availability Statement

The data that support the findings of this study are available in the supplementary material of this article.

**Keywords:** amphiphiles · charged  $\pi$ -electronic systems · ion-pairing assemblies ·  ${}^i\pi\text{-}^j\pi$  interactions · liquid crystals

- [1] Selectivity of solvents: a) S. Khoshkhoo, J. Anwar, *J. Phys. D* **1993**, *26*, B90–B93; b) L. Rajput, K. Biradha, *J. Mol. Struct.* **2011**, *991*, 97–102.
- [2] Aggregates dispersed in solutions: a) M. L. Lee, S.-J. Lee, L.-H. Jiang, *J. Am. Chem. Soc.* **2004**, *126*, 12724–12725; b) E. R. Zubarev, J. Xu, A. Sayyad, J. D. Gibson, *J. Am. Chem. Soc.* **2006**, *128*, 15098–15099; c) T. S. Kale, A. Klaikherd, B. Popere, S. Thayumanavan, *Langmuir* **2009**, *25*, 9660–9670; d) N. Fukaya, S. Ogi, H. Sotome, K. J. Fujimoto, T. Yanai, N. Bäumer, G. Fernández, H. Miyasaka, S. Yamaguchi, *J. Am. Chem. Soc.* **2022**, *144*, 22479–22492.
- [3] Selected reports: a) K.-S. Moon, H.-J. Kim, E. Lee, M. Lee, *Angew. Chem. Int. Ed.* **2007**, *46*, 6807–6810; *Angew. Chem.* **2007**, *119*, 6931–6934; b) Z. Huang, H. Lee, E. Lee, S.-K. Kang, J.-M. Nam, M. Lee, *Nat. Commun.* **2011**, *2*, 459.
- [4] D. Demus, J. Goodby, G. W. Gray, H.-W. Spiess, V. Vill, *Handbook of Liquid Crystals*, Wiley **1998**.
- [5] A review and first reports on lyotropic chromonic liquid crystals: a) A. Masters, *Liq. Cryst. Today* **2016**, *25*, 30–37; b) T. K. Attwood, J. E. Lydon, *Mol. Cryst. Liq. Cryst.* **1984**, *108*, 349–466; c) N. Boden, R. J. Bushby, L. Ferris, C. Hardy, F. Sixl, *Liq. Cryst.* **1986**, *1*, 109–125.
- [6] a) D. Görl, F. Würthner, *Angew. Chem. Int. Ed.* **2016**, *55*, 12094–12098; *Angew. Chem.* **2016**, *128*, 12273–12277; b) D. Görl, B. Soberats, S. Herbst, V. Stepanenko, F. Würthner, *Chem. Sci.* **2016**, *7*, 6786–6790; c) V. Grande, B. Soberats, S. Herbst, V. Stepanenko, F. Würthner, *Chem. Sci.* **2018**, *9*, 6904–6911.
- [7] a) A. Donval, E. Toussaere, S. Brasselet, J. Zyss, *Opt. Mater.* **1999**, *12*, 215–219; b) T. Schneider, O. D. Lavrentovich, *Langmuir* **2000**, *16*, 5227–5230.
- [8] a) G. J. Clarkson, B. M. Hassan, D. R. Maloney, N. B. McKeown, *Macromolecules* **1996**, *29*, 1854–1856; b) J. E. Halls, R. W. Bourne, K. J. Wright, L. I. Partington, M. G. Tamba, Y. Zhou, T. Ramakrishnappa, G. H. Mehl, S. M. Kelly, J. D. Wadhawan, *Electrochem. Commun.* **2012**, *19*, 50–54.
- [9] C. Rodríguez-Abreu, Y. V. Kolen'ko, K. Kovnir, M. Sanchez-Dominguez, R. G. Shrestha, P. Bairo, K. Ariga, L. K. Shrestha, *Phys. Chem. Chem. Phys.* **2020**, *22*, 23276–23285.
- [10] a) W. Lu, Y. Chen, V. A. L. Roy, S. S.-Y. Chui, C.-M. Che, *Angew. Chem. Int. Ed.* **2009**, *48*, 7621–7625; *Angew. Chem.* **2009**, *121*, 7757–7761; b) D. Pucci, B. S. Mendiguchia, C. M. Tone, E. I. Szerb, F. Ciuchi, M. Gao, M. Ghedini, A. Crispini, *J. Mater. Chem. C* **2014**, *2*, 8780–8788.

- [11] Recent reviews: a) K. Yamasumi, H. Maeda, *Bull. Chem. Soc. Jpn.* **2021**, *94*, 2252–2262; b) Y. Haketa, K. Yamasumi, H. Maeda, *Chem. Soc. Rev.* **2023**, *52*, 7170–7196.
- [12]  ${}^i\pi$ - ${}^i\pi$  Interactions for assemblies: Y. Sasano, H. Tanaka, Y. Haketa, Y. Kobayashi, Y. Ishibashi, T. Morimoto, R. Sato, Y. Shigeta, N. Yasuda, T. Asahi, H. Maeda, *Chem. Sci.* **2021**, *12*, 9645–9657.
- [13] Selected examples: a) Y. Haketa, S. Sasaki, N. Ohta, H. Masunaga, H. Ogawa, N. Mizuno, F. Araoka, H. Takezoe, H. Maeda, *Angew. Chem. Int. Ed.* **2010**, *49*, 10079–10083; *Angew. Chem.* **2010**, *122*, 10277–10281; b) B. Dong, T. Sakurai, Y. Honsho, S. Seki, H. Maeda, *J. Am. Chem. Soc.* **2013**, *135*, 1284–1287; c) B. Dong, T. Sakurai, Y. Bando, S. Seki, K. Takaishi, M. Uchiyama, A. Muranaka, H. Maeda, *J. Am. Chem. Soc.* **2013**, *135*, 14797–14805; d) Y. Bando, Y. Haketa, T. Sakurai, W. Matsuda, S. Seki, H. Takaya, H. Maeda, *Chem. Eur. J.* **2016**, *22*, 7843–7850; e) K. Yamasumi, K. Ueda, Y. Haketa, Y. Hattori, M. Suda, S. Seki, H. Sakai, T. Hasobe, R. Ikemura, Y. Imai, Y. Ishibashi, T. Asahi, K. Nakamura, H. Maeda, *Angew. Chem. Int. Ed.* **2023**, *62*, e202216013; *Angew. Chem.* **2023**, *135*, e202216013.
- [14] a) Y. Haketa, Y. Bando, Y. Sasano, H. Tanaka, N. Yasuda, I. Hisaki, H. Maeda, *iScience* **2019**, *14*, 241–256; b) H. Tanaka, Y. Kobayashi, K. Furukawa, Y. Okayasu, S. Akine, N. Yasuda, H. Maeda, *J. Am. Chem. Soc.* **2022**, *144*, 21710–21718.
- [15] a) O. W. Webster, *J. Am. Chem. Soc.* **1965**, *87*, 1820–1821; b) T. Sakai, S. Seo, J. Matsuoka, Y. Mori, *J. Org. Chem.* **2013**, *78*, 10978–10985.
- [16] S. H. Jung, H.-J. Kim, *J. Porphyrins Phthalocyanines* **2008**, *12*, 109–115.
- [17] The absorbance of  ${}^i\mathbf{1au}^+$ -PCCp $^-$  was decreased from that in  $\text{CH}_2\text{Cl}_2$ , although  ${}^i\mathbf{1au}^+$ -Cl $^-$  showed comparable absorbances in these solvents. In addition, the speculated arrangements of the charged  $\pi$ -electronic systems are not consistent with the theoretical estimations based on the transition dipole moment. The details on the correlation between spectroscopic behaviors and assembling modes will be discussed elsewhere. M. J. Frisch, G. W. Trucks, H. B. Schlegel, G. E. Scuseria, M. A. Robb, J. R. Cheeseman, G. Scalmani, V. Barone, G. A. Petersson, H. Nakatsuji, X. Li, M. Caricato, A. V. Marenich, J. Bloino, B. G. Janesko, R. Gomperts, B. Mennucci, H. P. Hratchian, J. V. Ortiz, A. F. Izmaylov, J. L. Sonnenberg, D. Williams-Young, F. Ding, F. Lipparini, F. Egidi, J. Goings, B. Peng, A. Petrone, T. Henderson, D. Ranasinghe, V. G. Zakrzewski, J. Gao, N. Rega, G. Zheng, W. Liang, M. Hada, M. Ehara, K. Toyota, R. Fukuda, J. Hasegawa, M. Ishida, T. Nakajima, Y. Honda, O. Kitao, H. Nakai, T. Vreven, K. Throssell, J. A. Montgomery Jr., J. E. Peralta, F. Ogliaro, M. J. Bearpark, J. J. Heyd, E. N. Brothers, K. N. Kudin, V. N. Staroverov, T. A. Keith, R. Kobayashi, J. Normand, K. Raghavachari, A. P. Rendell, J. C. Burant, S. S. Iyengar, J. Tomasi, M. Cossi, J. M. Millam, M. Klene, C. Adamo, R. Cammi, J. W. Ochterski, R. L. Martin, K. Morokuma, O. Farkas, J. B. Foresman, D. J. Fox, *Gaussian 16*, Revision C.01, Gaussian, Inc., Wallingford CT **2016**.
- [18]  ${}^i\mathbf{1au}^+$ -B(C $_6$ F $_5$ ) $_4^-$  showed the similar spectroscopic behavior to that of  ${}^i\mathbf{1au}^+$ -Cl $^-$ . The details will be discussed elsewhere.
- [19] Upon cooling, multiple Col $_h$   $a$  values were observed at 3.12, 3.05, 2.93, and 2.83 nm at 5 °C via synchrotron XRD.
- [20] Highly ordered assembly exhibiting LCST behavior: K. V. Rao, D. Miyajima, A. Nihonyanagi, T. Aida, *Nat. Chem.* **2017**, *9*, 1133–1139.
- [21] Selected examples of macroscopically oriented columnar assemblies: a) M. Yoshio, T. Kagata, K. Hoshino, T. Mukai, H. Ohno, T. Kato, *J. Am. Chem. Soc.* **2006**, *128*, 5570–5577; b) G. Schweicher, G. Gbabode, F. Quist, O. Debever, N. Dumont, S. Sergeev, Y. H. Geerts, *Chem. Mater.* **2009**, *21*, 5867–5874; c) X. Feng, M. E. Tousley, M. G. Cowan, B. R. Wiesenauer, S. Nejati, Y. Choo, R. D. Noble, M. Elimelech, D. L. Gin, C. O. Osuji, *ACS Nano* **2014**, *8*, 11977–11986; d) C. Li, J. Cho, K. Yamada, D. Hashizume, F. Araoka, H. Takezoe, T. Aida, Y. Ishida, *Nat. Commun.* **2015**, *6*, 8418.
- [22] Selected examples of single-stranded assemblies: a) P. Rajdev, S. Chakraborty, M. Schmutz, P. Mesini, S. Ghosh, *Langmuir* **2017**, *33*, 4789–4795; b) V. C.-H. Wong, C. Po, S. Y.-L. Leung, A. K.-W. Chan, S. Yang, B. Zhu, X. Cui, V. W.-W. Yam, *J. Am. Chem. Soc.* **2018**, *140*, 657–666; c) C. Otsuka, S. Takahashi, A. Isobe, T. Saito, T. Aizawa, R. Tsuchida, S. Yamashita, K. Harano, H. Hanayama, N. Shimizu, H. Takagi, R. Haruki, L. Liu, M. J. Hollamby, T. Ohkubo, S. Yagai, *J. Am. Chem. Soc.* **2023**, *145*, 22563–22576; d) Q. Liu, T. Zhang, Y. Ikemoto, Y. Shinozaki, G. Watanabe, Y. Hori, Y. Shigeta, T. Midorikawa, K. Harano, Y. Sagara, *Small* **2024**, *20*, 2400063.
- [23] A review: C. Tschierske, *Prog. Polym. Sci.* **1996**, *21*, 775–852.

Manuscript received: August 8, 2024

Accepted manuscript online: September 23, 2024

Version of record online: November 6, 2024